

ActA and human zyxin harbour Arp2/3-independent actin-polymerization activity

Julie Fradelizi*†, Vincent Noireaux†‡§, Julie Plastino‡, Bernadette Menichi*, Daniel Louvard*, Cécile Sykes‡, Roy M. Golsteyn*||¶ and Evelyne Friederich*¶#★**

*Laboratoire de Morphogenèse et Signalisation Cellulaires, Unité Mixte de Recherche CNRS/Institut Curie (UMR144) 26 rue d'Ulm, 75248 Paris cedex 05, France

‡Laboratoire Physico-Chimie Curie, Unité Mixte de Recherche CNRS/Institut Curie (UMR168), 26 rue d'Ulm, 75248 Paris cedex 05, France

★Laboratoire Franco-Luxembourgeois de Recherche Biomédicale, CNRS/CRP-Santé, Centre Universitaire, 162A, av. de la Faïencerie, L-1511, Luxembourg

§Current address: The Rockefeller University, Center for Studies in Physics and Biology, Box 265, 1230 York Avenue, New York, NY 10021, USA

||Current address: Division de Cancérologie Expérimentale, Institut de Recherches Servier, 125, chemin de Ronde, 78290 Croissy-sur-Seine, France

¶Current address: CRP-Santé, 18 rue Dicks, L-1417, Luxembourg

†These authors contributed equally to this work

#These authors share last authorship

**e-mail: evelyne.friederich@crp-sante.lu; roy.golsteyn@fr.netgrs.com

The actin cytoskeleton is a dynamic network that is composed of a variety of F-actin structures. To understand how these structures are produced, we tested the capacity of proteins to direct actin polymerization in a bead assay *in vitro* and in a mitochondrial-targeting assay in cells. We found that human zyxin and the related protein ActA of *Listeria monocytogenes* can generate new actin structures in a vasodilator-stimulated phosphoprotein-dependent (VASP) manner, but independently of the Arp2/3 complex. These results are consistent with the concept that there are multiple actin-polymerization machines in cells. With these simple tests it is possible to probe the specific function of proteins or identify novel molecules that act upon cellular actin polymerization.

The organization of the actin cytoskeleton in cells correlates strongly with the spatial organization of actin interacting proteins^{1–3}. This indicates that actin polymerization in cells may be controlled by distinct families of proteins, although the only cellular actin-polymerization complex identified to date is the Arp2/3 complex. Studies of the actin-dependent movement of *L. monocytogenes*⁴ have been instrumental in dissecting the role of the Arp2/3 complex in actin polymerization. In cells, the Arp2/3 complex cooperates with members of the family of Wiskott–Aldrich–syndrome protein (WASP) to nucleate actin filaments^{5,6} in Y-branched structures^{7,8}. This type of F-actin structure is present at the leading edge of the lamellipodia of human cells^{8,9}. As many F-actin structures in the cell are not organized into Y-shaped structures, it is reasonable to propose that cells contain other F-actin-organizing systems, although their identity is not yet known.

Whereas the amino-terminal domain of ActA^{10,11} harbours similar activity to the WA/VCA domain of WASP and related proteins, the proline-rich domain of ActA, known as ActA-Pro, harbours similar activity to the 380 amino acids at the amino terminus of human zyxin¹². Zyxin is the prototype of a family of proteins that is located at actin-rich sites in cells of higher eucaryotes^{13,14}. Members of this family, including zyxin^{15,16}, LPP (LIM-containing lipoma preferred partner)¹⁷ and TRIP6 (thyroid receptor-interacting protein-6)¹⁸, contain a proline-rich N-terminal domain followed by three LIM domains. Within the proline-rich domains of both ActA and zyxin are a series of FPPPP amino-acid repeats that are necessary for binding to vasodilator-stimulated phosphoprotein (VASP)^{19,20}. Disruption of the interaction between ActA and VASP causes *L. monocytogenes* to move more slowly^{21,22}. Furthermore, VASP is not essential for *L. monocytogenes* movement *in vitro*, although when it is added to reconstituted extracts, it increases the rate of bacterial movement²³.

To identify new cellular actin-polymerization systems, we used two different assays: a bead system, using recombinant proteins to

examine actin polymerization under controlled conditions in cell-free extracts, and a permeabilized cell system, to examine actin polymerization under cellular conditions. Here we show that beads coated with either of the related proteins, ActA-Pro or zyxin, can polymerize actin in cell-free extracts *in vitro*, and that human zyxin harbours actin-polymerization activity under cellular conditions by expressing zyxin at the surface of mitochondria. These activities are distinct from the actin-polymerization activity of the Arp2/3/WASP family of proteins, as shown by immunolocalization and inhibitor studies. These findings lead us to propose that cells harbour several distinct actin-polymerization complexes, which together contribute to the dynamics of the actin cytoskeleton.

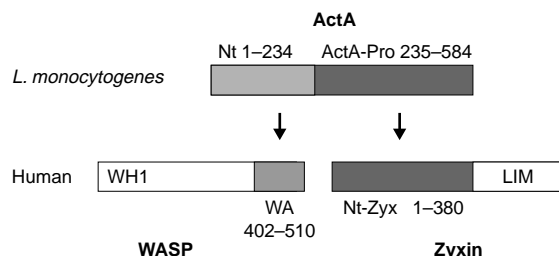


Figure 1 Structural features of the ActA, WASP and zyxin proteins. The 234 amino acids at the N terminus of ActA have an Arp2/3-dependent nucleating activity which is similar to that found within the WA domain (100 amino acids) of WASP. Similarly, the C-terminal ActA-Pro domain of ActA is reported to interact with the actin cytoskeleton in a similar manner to the N-terminal proline-rich domain of human zyxin. The function of ActA-Pro and zyxin were then tested in the bead and mitochondria actin-polymerization assays.

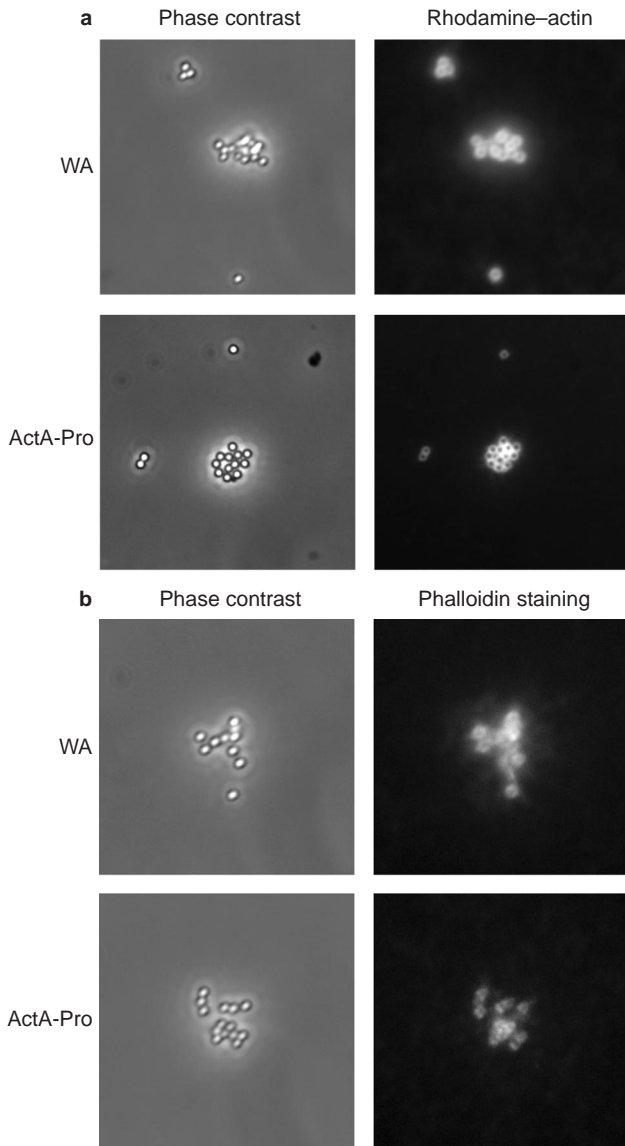


Figure 2 ActA-Pro-coated beads promote actin polymerization in cell-free extracts. **a**, Beads (500 nm) coated with either WA or ActA-Pro proteins were incubated in HeLa cell extracts that were supplemented with actin labelled with fluorochrome (1 μ M). Samples were removed for observation by phase-contrast (left panels) and fluorescence (right panels) microscopy. Both WA and ActA-Pro beads were labelled with actin, indicating that they support actin polymerization. **b**, Beads (500 nm) coated with either WA or ActA-Pro proteins were incubated in HeLa cell extracts for at least 30 min before addition of rhodamine-labelled phalloidin. Samples were removed for observation by phase-contrast (left panels) and fluorescence (right panels) microscopy. Both WA and ActA-Pro beads were stained by phalloidin, indicating that they were covered with F-actin.

Results

To identify new systems of cellular actin polymerization, we focused on the proteins ActA-Pro and zyxin and compared their function to WASP in a bead-based actin-polymerization assay. The functional relationships between ActA, ActA-Pro, WA and zyxin are shown in Fig. 1. We used an epitope-tagged WA protein²⁴. WA protein or ActA-Pro proteins were absorbed to solid latex beads that were added to cell-free extracts prepared from cultured HeLa cells. The presence of each protein on the surface of beads was confirmed by antibody staining and immunofluorescence microscopy (data

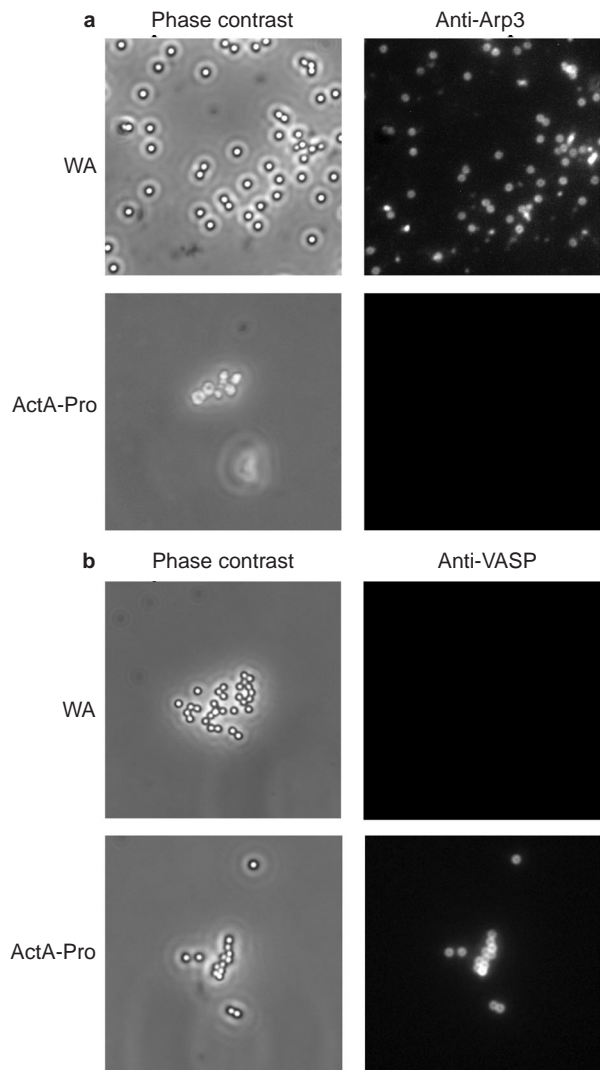


Figure 3 The Arp2/3 complex is not recruited to the surface of ActA-Pro beads. **a, b**, Beads coated with either WA or ActA-Pro proteins were incubated in HeLa cell extracts in the presence of latrunculin A, and then treated with either anti-Arp3 antibodies (**a**) or anti-VASP antibodies (**b**). Antibody binding was detected by fluorescently tagged secondary antibodies, and samples were removed for observation by phase-contrast (left panels) and fluorescence (right panels) microscopy. The absence of staining by anti-Arp3 antibody indicated that ActA-Pro polymerizes actin independently of the Arp2/3 complex.

not shown). To detect actin polymerization, actin labelled with the fluorochrome Alexa 568 was added to the extracts (ratio of unlabelled to labelled actin, 19/1 μ M). WA and ActA-Pro beads were visible by fluorescence, indicating that both beads recruit G-actin in these extracts (Fig. 2a). A weaker signal was observed with ActA-Pro beads. This might be because ActA-Pro polymerizes actin more slowly than WA (Fig. 4). In a related test, WA and ActA-Pro beads were added to cell extracts without additional actin. Both WA and ActA-Pro beads were labelled by phalloidin, revealing that they were coated with F-actin at their surface (Fig. 2b). When tested under similar conditions, beads coated with either bovine serum albumin (BSA) or glutathione S-transferase (GST) did not recruit either G-actin or F-actin (data not shown). To determine whether the actin recruited by WA and ActA-Pro beads was from a dynamic or a stable cellular pool, extracts containing actin labelled with Alexa 568 were treated with either various concentrations of

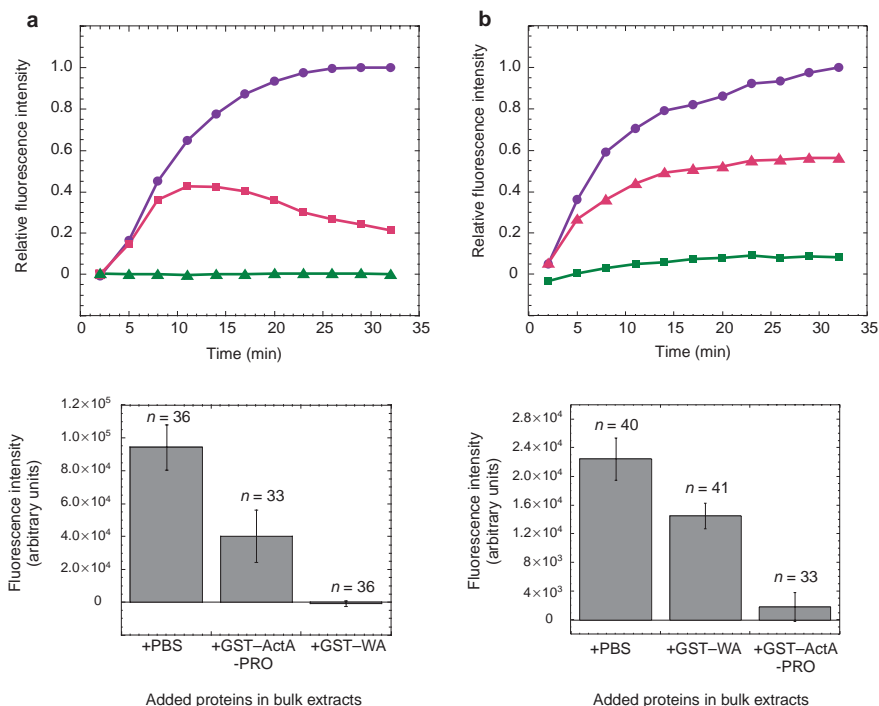


Figure 4 ActA-Pro-directed actin polymerization is independent of the Arp2/3 complex. **a, b,** Beads (10 μm) coated with either WA (**a**) or ActA-Pro (**b**) proteins were incubated in HeLa cell extracts that were supplemented with actin conjugated to Alexa 568 (1 μM). The fluorescence signal was monitored by video microscopy. WA beads were incubated in the presence of buffer only (circles), ActA-Pro (1 mg ml^{-1} ; squares) or exogenous WA protein (1 mg ml^{-1} ; triangles) and the recruitment of actin was monitored (**a**, top panel). The average fluorescent signals after 1 h incubation and error bars are shown from measurements of at least 33 beads in each case (**a**, lower panel).

Acta-Pro beads were incubated in the presence of buffer only (circles), WA protein (1 mg ml^{-1} ; triangles) or exogenous ActA-Pro (1 mg ml^{-1} ; squares), and the recruitment of actin was monitored (**b**, top panel). The average fluorescent signals after 1 h incubation and error bars are shown from measurements of at least 33 beads in each case (**b**, lower panel). Note that ActA-pro-directed actin polymerization can continue in the presence of WA protein that competes for Arp2/3-dependent actin polymerization.

latrunculin A or 2 μM of cytochalasin D before the beads were added. In the presence of either of these drugs, the recruitment of actin at the bead surface of both bead types was highly reduced, indicating that the recruitment of actin was a dynamic process. The reduction in polymerization observed in the presence of cytochalasin D was not due to increased ATPase activity of actin. (see Supplementary Information). Latrunculin A reduced actin polymerization at the bead surfaces in a dose-dependent manner, as expected from a sequestering agent (100% inhibition with 4 μM latrunculin A for both bead types).

Although the WA and ActA-Pro beads displayed a capacity to recruit actin, it was not clear whether these processes use the same molecular pathway. To test this, we probed the beads incubated in extracts in the presence of latrunculin A with anti-Arp3 antibodies to detect the Arp3 protein, a component of the Arp2/3 complex that is necessary for WA-dependent actin polymerization. As expected, the WA beads were stained by anti-Arp3 antibody after incubation in cell-free extracts. However, ActA-Pro beads did not have any Arp3 staining, even though these beads were capable of producing actin filaments (Fig. 3a). In contrast, WA beads were not stained by anti-VASP antibodies, a protein that binds to the proline-rich domains of ActA and of human zyxin, whereas ActA-Pro beads were readily stained by this antibody (Fig. 3b). These results indicate that ActA-Pro beads recruit actin by a mechanism that is independent of the Arp2/3 complex and may require VASP. We also tested Arp3 and VASP staining in the absence of latrunculin A to investigate the indirect recruitment of these proteins by actin filaments (see Supplementary Information). Although an almost identical result was obtained with Arp3 antibody, VASP staining was significantly

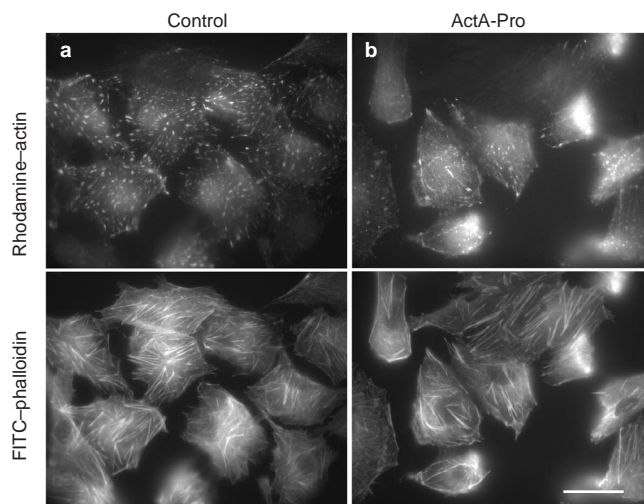


Figure 5 ActA-Pro reduces actin polymerization at cell-adhesion sites. **a, b,** Vero cells were permeabilized and then incubated with rhodamine-actin (0.4 μM) for 5 min in the absence (**a**) or presence (**b**) of ActA-Pro-GST (0.25 mg ml^{-1}). After fixation, cells were stained with FITC-phalloidin to visualize F-actin structures. In control cells, rhodamine-actin incorporated at sites that correspond to focal adhesions and stress fibres (**a**). When cells were incubated in the presence of ActA-Pro protein (**b**), actin incorporation at these sites was highly reduced. Scale bar, 20 μm .

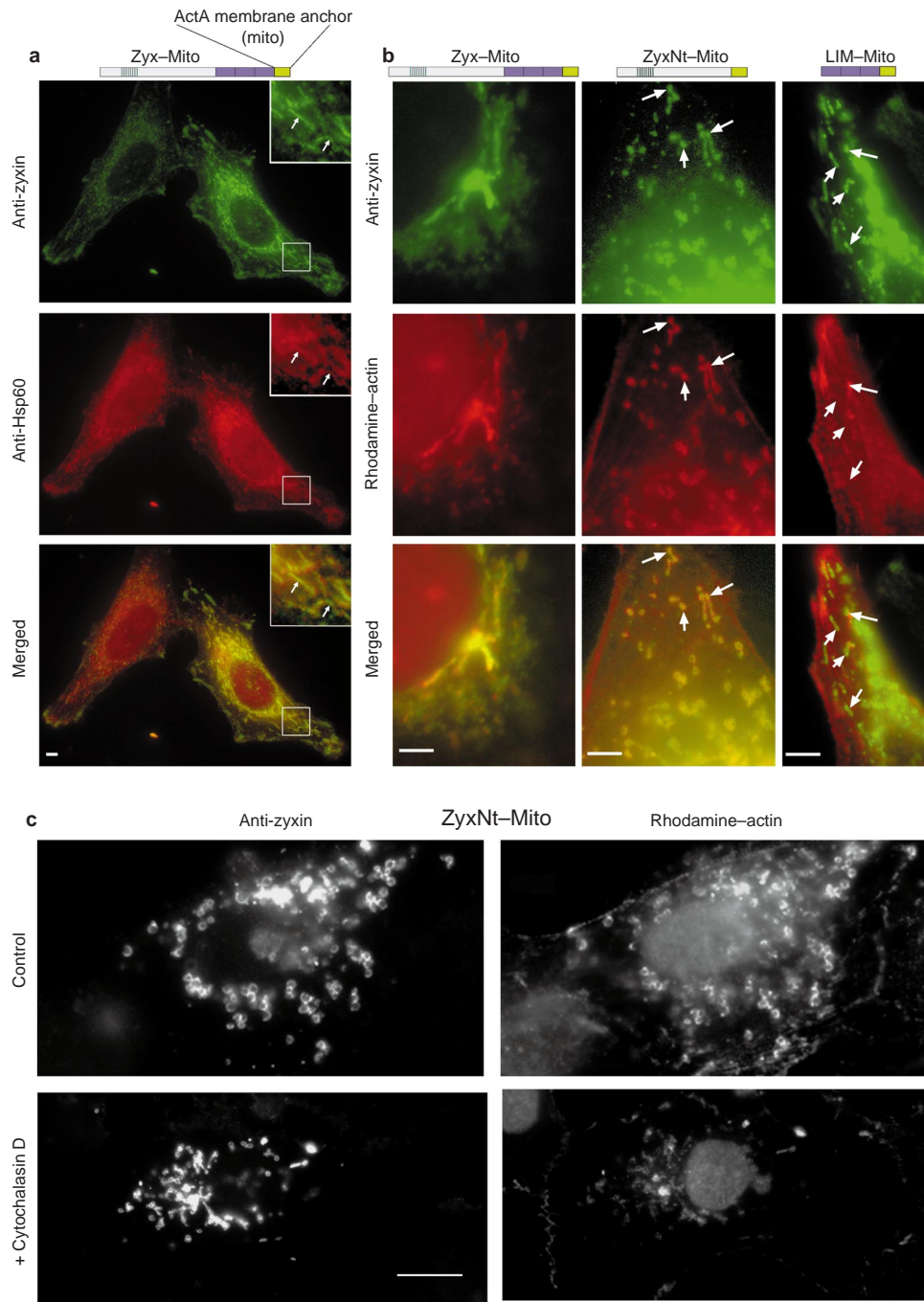


Figure 6 The proline-rich domain of zyxin mediates actin polymerization in cells. DNA constructs used for transfection are represented above the fluorescence-microscopy images. **a**, Permeabilized HeLa cells transiently transfected with Zyx-Mito were stained with anti-zyxin antibodies (top panel, green) or anti-hsp60 antibodies as a probe for mitochondria (middle panel, red). Insets, higher magnification of cell areas highlighted by squares to show co-distribution of anti-zyxin and anti-hsp60 labels (arrows). The lower panel represents a merged image of top and middle panels. **b**, HeLa cells, transiently transfected and permeabilized, were incu-

bated with actin coupled with rhodamine (0.4 μ m) for 5 min, fixed and labelled with anti-zyxin antibodies. Top panels, zyxin staining (green); middle panels, rhodamine-actin incorporation (red); lower panels, merged images. Note that ZyxNt-Mito but not LIM-Mito co-distributes with rhodamine-actin label (arrows). **c**, Vero cells transiently transfected with ZyxNt-Mito were pretreated with permeabilization buffer for 3 min in the presence of 100 nM cytochalasin D, and then incubated for 4 min in the presence of 0.4 μ M rhodamine-actin and 100 nM cytochalasin D. Scale bars, 5 μ m.

increased with WA beads. To confirm that actin polymerization by ActA-Pro beads was not dependent on the Arp2/3 complex, we inhibited Arp2/3-dependent polymerization on WA-coated beads by adding WA protein in solution to the extracts to compete with WA beads for this complex. The WA domain of Scar protein can

compete with ActA for binding to the Arp2/3 complex, thereby inhibiting Arp2/3-dependent actin polymerization at the surface of *L. monocytogenes*²⁵. In the presence of exogenous WA protein, no actin polymerization was detected on WA beads, indicating that Arp2/3-dependent actin polymerization had been inhibited

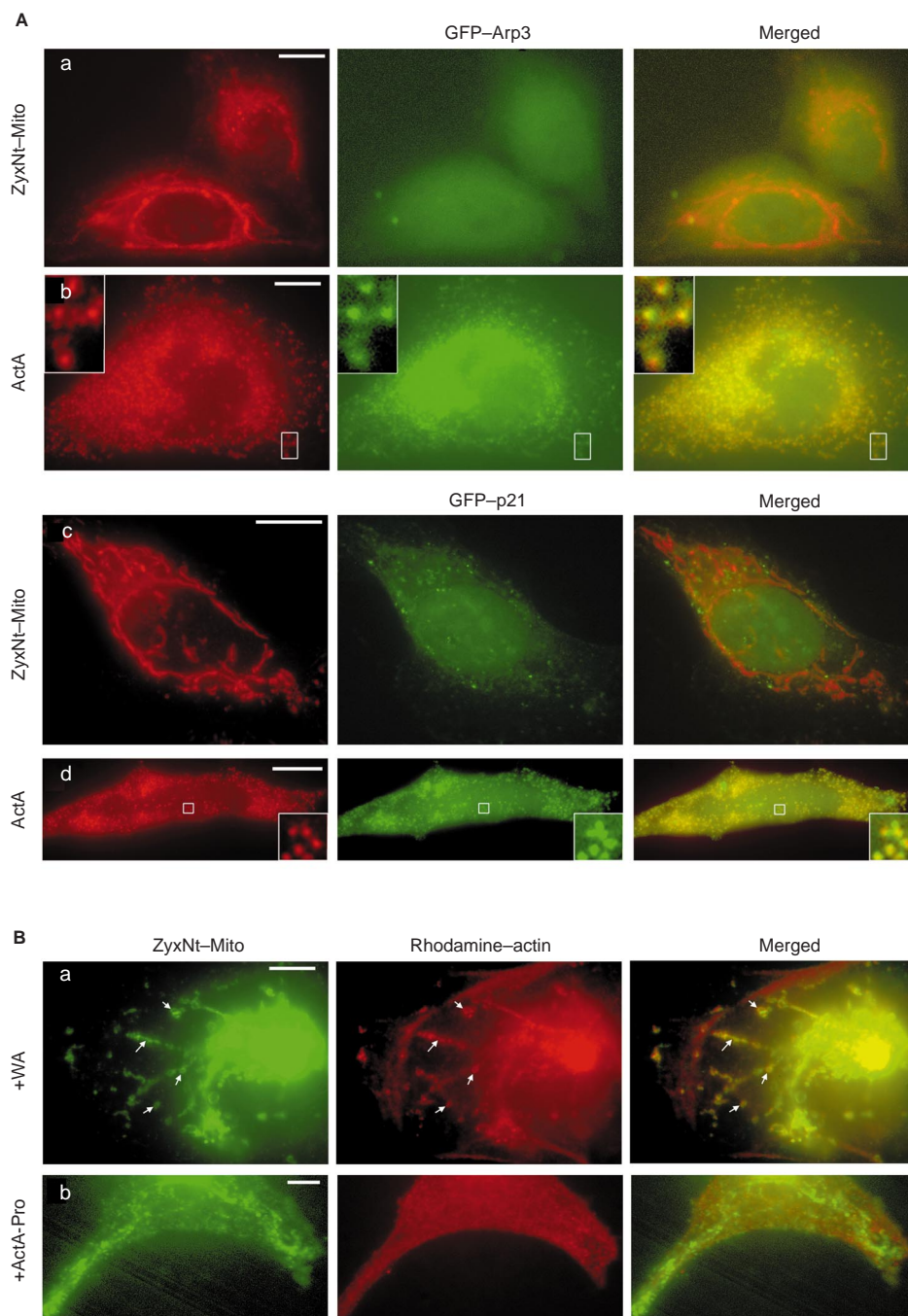


Figure 7 Zyxin-mediated actin polymerization is independent of the Arp2/3 complex. **Aa–d**, HeLa cells were co-transfected either with ZyxNt-Mito and GFP-Arp3 (**a**) or GFP-p21 (**c**), or with ActA and GFP-Arp3 (**b**) or GFP-p21 (**d**). The cells were fixed and examined for co-localization. Left panels, immunofluorescence staining of zyxin or ActA (red); middle panels, GFP fluorescence; right panels, merged images of left and middle images. Although no localization was observed

with ZyxNt-Mito (**a**, **c**, merged images), ActA at the mitochondria co-localizes with components of the Arp2/3 complex (**b**, **d**, merged images). Inserts, higher magnifications of cell areas highlighted by squares to show co-distribution of ActA label and GFP-Arp3 (**b**) or GFP-p21 (**d**) fluorescence. **Ba**, **b**, HeLa cells transiently transfected with ZyxNt-Mito were treated as for Fig. 6B but with the addition of either WA protein (1 mg ml⁻¹; **a**) or ActA-Pro (1 mg ml⁻¹; **b**).

(Fig. 4a). However, ActA-Pro beads continued to polymerize actin in the presence of WA protein, albeit at a reduced rate (Fig. 4b). This is probably because WA-mediated actin polymerization in solution reduces the G-actin pool available for actin polymerization. Similarly, we measured the capacity of WA and ActA-Pro beads to polymerize actin in the presence of exogenous ActA-Pro protein. Under these conditions, ActA-Pro beads no longer polymerized

actin, whereas WA beads continued to polymerize, but less extensively than in samples without any added protein (Fig. 4a). These results indicate that ActA-Pro beads may polymerize actin by a mechanism that is independent of the Arp2/3 complex.

The ActA-Pro subdomain, which displays actin-polymerization properties in the bead assay, shares sequence and functional properties with the human zyxin protein. Latex beads coated with a

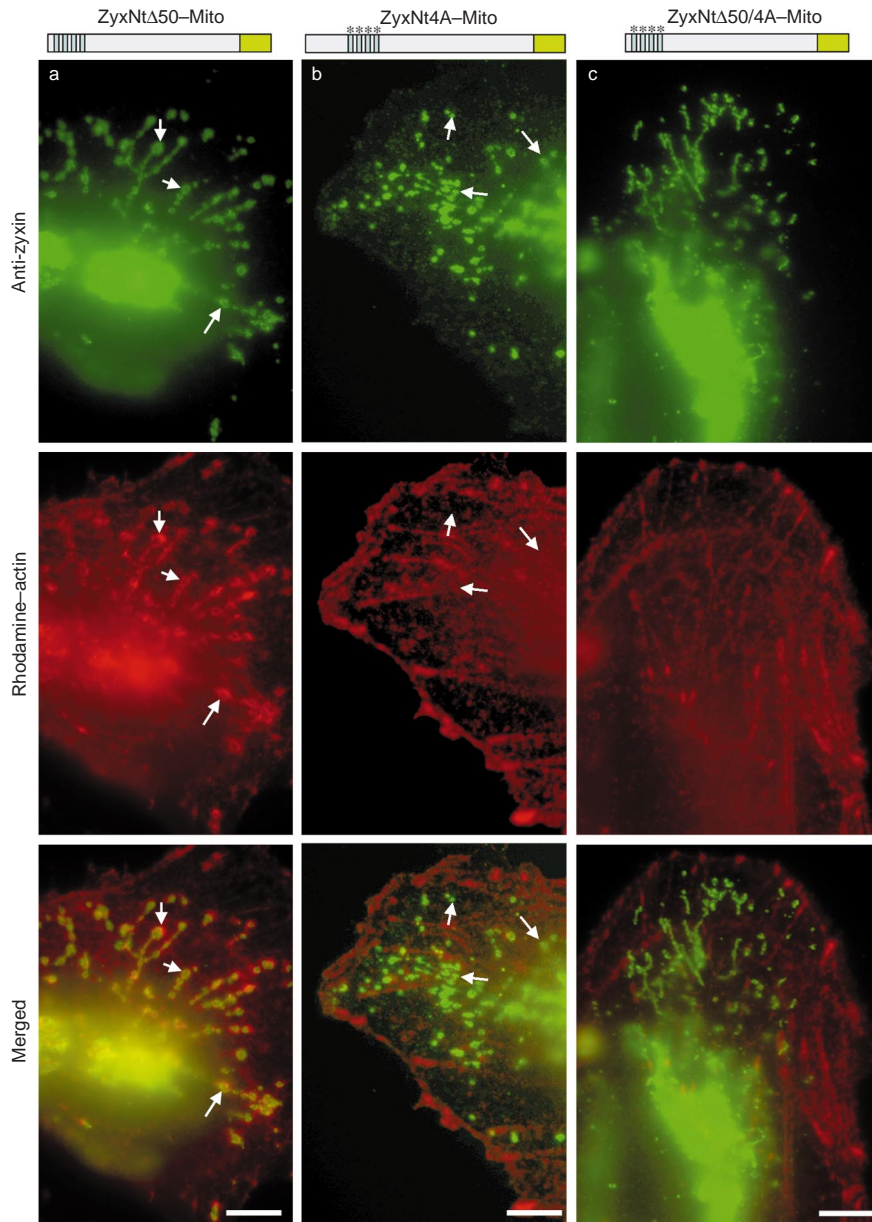


Figure 8 Zyxin-mediated actin polymerization is dependent on VASP. a–c. HeLa cells transiently transfected with *zyxNtΔ50-Mito* (a), *zyxNt4A-Mito* (b) or *zyxNtΔ50/4A-Mito* (c) were treated as for Fig. 6B. Upper panels, zyxin staining

(green); middle panels, rhodamine-actin incorporation (red); lower panels, merged images. Arrows point to distinct mitochondrial structures that are covered by zyxin variants.

series of zyxin peptide fragments, isolated from recombinant bacteria as previously described²⁶, were positive for actin polymerization in cell-free extracts (data not shown). This result prompted us to examine the actin-polymerization properties of zyxin in cells. Zyxin and zyxin-related proteins such as LPP are enriched at focal contacts, which are sites that display actin-polymerization activity. To examine the proteins required for actin polymerization at focal contacts in cells, we incubated permeabilized cells with actin labelled with rhodamine in the presence of ActA-Pro protein (Fig. 5). In control cells, rhodamine-actin was incorporated into focal adhesions and stress fibres, as visualized by double-staining of cells with fluorescein isothiocyanate (FITC)-phalloidin (Fig. 5a). Addition of ActA-Pro protein to permeabilized cells very much reduced actin incorporation at these sites in 90% of the analysed cells, although some staining was still visible along the plasma

membrane (Fig. 5b). These results indicate that some forms of cellular actin polymerization are dependent on a protein that resembles the protein ActA-Pro, of which the human protein zyxin is a likely candidate. We tested this hypothesis by examining the role of zyxin in actin polymerization in permeabilized cells.

To test the properties associated with actin polymerization of zyxin, the protein was placed at the surface of mitochondria, away from typical actin-rich sites in cells; this approach had been used to study the interaction of α -actinin and zyxin²⁶. Cells transfected with cDNAs-encoding zyxin variants were permeabilized with saponin and incubated with rhodamine G-actin. The localization of full-length zyxin with a membrane anchor (*Zyx-Mito*) was confirmed by co-localization studies with Hsp60 protein, a component of the outer membrane of mitochondria (Fig. 6a). Cells that expressed *zyx-Mito* incorporated G-actin at the mitochondrial

surface (Fig. 6b), whereas control cells did not (data not shown). To identify the subdomains of zyxin that were responsible for actin recruitment, we then expressed zyxin variants containing the N-terminal domain (ZyxNt-Mito) or the three LIM domains of zyxin (LIM-Mito). Only the cells that produced ZyxNt-Mito had actin structures at the mitochondrial surface, indicating that the proline-rich domain of zyxin may have actin-recruiting activity, which is consistent with what was identified with the Act-Pro beads in cell-free extracts. In experiments in which permeabilized cells were incubated with 100 nM cytochalasin D, the incorporation of rhodamine-labelled G-actin at the mitochondria was markedly reduced (Fig. 6c), indicating that the production of F-actin was due to polymerization rather than the recruitment of actin filaments. In each case, the mitochondria that incorporated actin at their surface were also stained by rhodamine-labelled phalloidin (in the absence of rhodamine-labelled G-actin; data not shown), revealing that F-actin was produced.

We then tested whether the Arp2/3 complex participates in the incorporation of actin by mitochondrial-targeted zyxin. HeLa cells were co-transfected with cDNAs encoding ZyxNt-Mito and green fluorescent protein GFP-Arp3 or GFP-p21, which are components of the Arp2/3 complex, to enable the detection of the Arp2/3 complex in cells. Under these conditions, neither GFP-Arp3 nor GFP-p21 co-localized with ZyxNt-Mito (Fig. 7Aa, c), whereas the Arp2/3 complex was detected by this method in cells in which ActA was directed to the mitochondria (Fig. 7Ab, d). To confirm that zyxin-dependent actin structures do not require the Arp2/3 complex, we incubated cells with WA protein in the presence of actin labelled with rhodamine to inhibit actin polymerization stimulated by Arp2/3, as has been shown for *L. monocytogenes*. The incorporation of actin at the mitochondrial surface was not sensitive to WA protein (Fig. 7Ba), indicating that zyxin-dependent polymerization does not require the Arp2/3 complex, whereas the addition of exogenous ActA-Pro protein blocked zyxin-dependent actin polymerization (Fig. 7Bb).

When zyxin is directed to mitochondria, it retains its capacity to recruit α -actinin and VASP^{20,26}. Therefore, to identify the molecular mechanism by which ZyxNt-Mito generates actin structures, we prepared a mutant, zynNt Δ 50-Mito, that abrogates the interaction of zyxin with α -actinin, and a mutant, ZyxNt4A-Mito, that abrogates the interaction of zyxin with VASP^{20,26}. These mutants were tested for their capacity to polymerize actin at the mitochondrial surface. The ZyxNt Δ 50-Mito protein, in which the α -actinin-binding site is absent, did not recruit α -actinin but still retained its capacity to polymerize actin (Fig. 8a). In contrast, the variant ZyxNt4A-Mito, which does not recruit VASP, did not polymerize actin, indicating that the interaction between zyxin and VASP is necessary for actin-polymerization activity (Fig. 8b). The variant ZyxNt4A-Mito recruited F-actin through its α -actinin activity but this did not stimulate G-actin incorporation. In a subsequent test with a zyxin variant, ZyxNt Δ 50/4A-Mito, in which both α -actinin- and VASP-binding sites are compromised, actin structures were not found at mitochondrial surfaces after either phalloidin-staining (data not shown) or incorporation of G-actin (Fig. 8c). These results were consistent with a role for VASP and zyxin in cellular actin polymerization.

Discussion

The 380 amino acids at the N-terminal domain of zyxin has several biochemical and cell biological properties in common with the carboxy-terminal proline-rich domain of ActA, known as ActA-Pro^{10,19}. When placed on beads and added to cell-free extracts, ActA-Pro creates new actin structures by a mechanism that is independent of the Arp2/3 complex. Even though it is known that ActA polymerizes actin on beads^{27,28}, it has been assumed that all actin-polymerization activity arises from the 234 amino acids at the N terminus of ActA through its interaction with the Arp2/3 complex^{29,30},

presumably in a WASP-like manner²⁵. On the basis of the data described here, we propose that ActA-Pro polymerizes actin in a manner that is distinct from the N terminus of ActA. Therefore, ActA is composed of two rather than one actin-polymerization systems.

We do not know how these two polymerization systems are integrated; however, analysis of *L. monocytogenes* ActA mutants, in which the ActA-Pro subdomain is eliminated or sequentially deleted, reveals that both systems are required for maximum bacterial movement and virulence^{21,22,28,31}. There are other data that would fit better with a model that predicts two actin-polymerization systems present in ActA. The origin of long, unbranched filaments in *L. monocytogenes* comets³², including comets present in cell protrusions³³ might be better explained by a second polymerization system operating in addition to the Arp2/3 complex that generates highly branched filaments^{8,34}. By analogy to the ActA system, such filaments may originate from an ActA-Pro-like system of actin polymerization.

The common polymerization properties found with ActA-Pro or zyxin on beads strongly supports the prediction that a zyxin-dependent actin polymerization might be present in eukaryotic cells³⁵. Furthermore, ActA-Pro disrupted actin recruitment at focal adhesion plaques, which is consistent with a specific role for zyxin in actin polymerization. Zyxin placed at the surface of mitochondria polymerized actin in a VASP-dependent manner which was not sensitive to the Arp2/3 complex. Although zyxin also recruited actin filaments through its interaction with α -actinin, as was reported elsewhere²⁶, this type of recruitment did not account for polymerization as the filaments were not marked by rhodamine-actin during the time course of the assay³⁶. Although it has been reported that VASP binds to F-actin *in vitro* at very low salt conditions³⁷, it is improbable that the VASP-dependent actin polymerization that we report here corresponds to binding of F-actin. F-actin structures dependent upon VASP were marked by rhodamine-actin, whereas F-actin structures dependent upon α -actinin were not, showing that this assay can distinguish between polymerization of F-actin (VASP-dependent) and recruitment of F-actin (α -actinin dependent). In view of the capacity of zyxin to organize preformed filaments^{26,36} and to polymerize new filaments as shown here, it follows that zyxin is important for coordinating a subset of F-actin structures in cells²⁰. It remains to be determined whether VASP-dependent actin polymerization occurs through nucleation or uncapping of actin filaments.

We showed that WA-directed actin polymerization is distinct from ActA-Pro- or zyxin-directed polymerization by using immunolocalization and inhibition studies. In cells, however, these two systems are probably coordinated through signalling pathways or by the participation of associated proteins. One protein that is common to both systems is profilin that interacts with actin³⁸, VASP³⁹ and the Arp2/3 complex⁴⁰. The two systems may also interact in a structural manner, with one type of actin filament contributing to the production of other types of actin filaments. Although it has not been tested directly, Arp2/3-dependent actin polymerization is enhanced by the addition of non-branched actin filaments, which presumably originate from other F-actin-organizing systems⁴¹.

The identification of a zyxin system of actin polymerization supports the concept of 'cellular actin polymerization', which is distinct from polymerization of pure actin *in vitro*. We propose that cellular actin polymerization unlocks the molecular mechanisms that block the inherent capacity of actin to polymerize in a concentration-dependent manner. For proper cell function, cellular actin polymerization is probably tightly regulated at four levels: location, filament organization, timing and rate. One of the main cellular locations of zyxin is at focal contacts³, which do not stain positive for the Arp2/3 complex¹. The organization of F-actin at these sites is distinct from that of the branched filaments at the leading edge of cells. We would thus predict that zyxin-dependent actin polymerization

would produce filaments in an arrangement similar to the parallel filaments that have been identified in *L. monocytogenes* comets. Unlike cytokinesis, or the production of a lamellipodia, the timing of actin structures that require zyxin is not yet well defined. However, in experiments in which new actin structures are produced, such as during cell spreading, zyxin/VASP interaction seems to be important²⁰. It has been observed that actin is recruited more readily at the leading edge than at focal adhesion sites in cells. Nonetheless, even if the rate of actin turnover with a zyxin-dependent system is slow relative to the Arp2/3/WASP system, as zyxin is present at 10⁶–10⁷ copies depending on the cell type, it is a major actin polymerization unit⁴².

By examining ActA-pro and zyxin in cell-free and cell-based assays, we were able to attribute a new cell-like actin-polymerizing activity to these proteins. The identification of this system indicates that cells might contain many actin-polymerization systems, each being responsible for a particular type of actin structure. To understand how the actin cytoskeleton functions in cells, it will be necessary to identify the contribution of each system. Furthermore, the simple assays described here can be used to study other candidate proteins of the actin cytoskeleton, and to identify novel inhibitors of each type of cellular actin polymerization. □

Methods

Cell culture.

The human cervix carcinoma HeLa cell line (ATCC CCL-2) and the monkey kidney fibroblastic Vero cell line were grown in DMEM supplemented with 2 mM glutamine and 10% fetal calf serum (with 10% CO₂ at 37 °C) on plastic dishes or in suspension.

Plasmid constructs.

Zyxin constructs were inserted into the pUHD10-3 vector, placing zyxin sequences in frame with a sequence encoding the 9E10 myc epitope tag (for Nter constructs) and a 3'-located sequence encoding the membrane anchor of ActA (LLAMLAIGVFLSGAFIKIIQLRKNN; kindly provided by P. Cossart). Zyx-Mito, ZyxNt-Mito, ZyxNtΔ50-Mito and LIM-Mito encode the amino acids 1-572, 1-380, 51-380 and 332-572 of zyxin, respectively. ZyxNt4A-Mito and ZyxNtΔ50/4A-Mito encode the same protein as ZyxNt-Mito and ZyxNtΔ50-Mito, respectively, with four codons changed from phenylalanine to alanine in VASP-binding sites. ZyxNt-Mito and ZyxNt4A-Mito constructs have been described²⁰. The expression of all zyxin variants was confirmed by western blotting (data not shown). GST-WA was prepared by amplifying by polymerase chain reaction a DNA fragment encoding the amino acids 404-502 of human WASP (kindly supplied by P. Chavrier), and subcloning into pGEX-2T plasmid. The sequence encodes 226 amino acids of GST in frame with the amino acids 404-502 of WASP followed by the sequence EQKLISEEDL, which is recognized by the anti-Myc antibody 9E10. GST-ActA-Pro was prepared and purified as described¹⁵.

Actin-polymerization bead assays.

Polystyrene beads (Polysciences) of 0.5-, 1.0- and 10-µm diameters were coated with either GST-WA or GST-ActA-Pro proteins to saturation according to the manufacturer's protocol. Protein binding was confirmed by staining the beads with anti-GST antibody or anti-Myc 9E10 antibody (data not shown). Before use, the coated beads were washed, resuspended and stored in PBS on ice. For video-microscopy experiments, beads were used within 12 h after preparation. Extracts were prepared from HeLa cells in a manner similar to that described for platelet, although cells were lysed by shearing in a cell cracker⁴³. Typically, 10¹⁰ cells were used to make 12 ml of extract at 17 mg ml⁻¹. The concentration of total actin in extracts was measured by quantitative western blotting as described⁴². The primary antibody was anti-human β-actin (Sigma) used in tenfold excess over manufacturer's suggestion. The secondary actin antibody was anti-mouse Cy5-coupled antibody (Jackson Laboratories) used also in tenfold excess. Actin standards, which were loaded on the same gels as the extracts, were prepared from human-platelet actin (Cytoskeleton) and were measured spectrophotometrically at 290 nm in G-actin buffer, assuming an extinction coefficient of 0.63 ml mg⁻¹ cm⁻¹. The total amount of actin in the extracts was 19.1 µM (0.8 mg ml⁻¹ in extracts of 17.0 mg ml⁻¹).

1% solid suspension (0.5 µl) was mixed to HeLa cell-free extracts (15 µl) supplemented with ATP (1 mM), creatine phosphate (30 mM) and actin coupled to rhodamine or Alexa 568 on lysine residues (1 µM (5% of total actin); Molecular Probes). 1.5 µl of PBS, GST-WA (1 mg ml⁻¹) or GST-ActA-Pro (1 mg ml⁻¹) were added to the extracts. The final mixtures (6 µl) were squashed on coverslips, sealed and observed by phase-contrast and fluorescence microscopy. In some experiments, cytochalasin D (final concentration, 2 µM), latrunculin A (final concentrations, 0.1–12 µM), or rhodamine-labelled phalloidin (final concentration, 1 µM) in the absence of fluorochrome-labelled actin were added. Recruitment of specific proteins was detected by incubation of the beads in extracts. In some experiments the extracts were supplemented with 2.5 µM latrunculin A to inhibit actin polymerization. Arp3 was detected by an affinity-purified anti-Arp3 antibody (a gift from E. Gouin and P. Cossart). Anti-VASP antibody (V40620) was purchased from Transduction Laboratories. Beads were stained with various antibodies as follows: anti-Arp3 antibody (10 µg ml⁻¹); anti-VASP antibody (1/50 dilution); anti-myc 9E10 antibody (1/10 dilution). Beads were washed with 0.2% Triton-X100 and 0.1% BSA in PBS (pH 7.0) before and after addition of secondary antibodies. For observation, 3 µl of suspension containing beads were loaded onto glass slides, coated with a coverslip, sealed with vasoline and observed

by fluorescence microscopy. Identical exposure times were used to acquire images of beads stained with the same antibodies. To observe actin recruitment over time, preparations were incubated in the dark at 20 °C for 1 h. Samples were observed by fluorescence microscopy with an inverted video microscope that provides linear signal (microscope, Leica DM IRBE, GmbH, BP 2040; lens, Leica immersion oil, × 100; camera: micromax model RTE/CCD-1300-Y, Princeton Instruments), and were analysed with MetaMorph version 3.51 software. Beads were illuminated for one second and signals (rhodamine-actin) from the images integrated after subtraction of the background. For graphs of actin dynamics, one bead was illuminated 1 s every 3 min; the first image was acquired 2 min after adding beads to the extracts containing 1 mg ml⁻¹ of either GST-WA or GST-ActA-Pro. At least 30 beads were observed for all experiments, and all the observed beads were chosen in the centre of the slides.

Transfections.

DNAs encoding fusions of full-length zyxin or zyxin variants with the ActA membrane anchor were transfected using the calcium phosphate DNA-precipitation method. pUHD 10-3 vector (2 µg), in which expression of the cDNA is under the control of a minimal promoter, were co-transfected with pUHD15-1 plasmid (2 µg) which encodes the tetracycline-dependent transactivator tTAs. Cells were analysed 24–48 h after addition of DNA. GFP-p21 and GFP-Arp3 cDNAs were a gift from L. Machesky.

Permeabilization assay.

Transfected HeLa or Vero cells were permeabilized for 2 min with 50 µl of permeabilization buffer (10 mM HEPES, pH 7.7, 100 mM KCl, 1 mM MgCl₂, 0.1 mM CaCl₂, 50 mM sucrose, 0.6 mg ml⁻¹ saponin, 1 mM ATP), and then for 5 min in the same buffer containing 0.4 µM rhodamine-actin labelled on lysine residues⁴⁴. Cytochalasin D (100 nM; Sigma) or proteins were added in the permeabilization buffer as indicated.

Analysis of cells by epifluorescence and confocal laser-scanning microscopy.

Permeabilized cells were processed for immunofluorescence as described⁴⁵. Texas-red phalloidin was used to visualize F-actin (Molecular Probes) and anti-Hsp60 (provided by C. Koehler) to visualize mitochondria. The affinity-purified anti-zyxin antibody was raised against a peptide derived from human zyxin (YAQQREKPRVEK). Cy2-coupled goat anti-rabbit and Texas-red-coupled goat anti-mouse IgG antibodies were purchased from Jackson ImmunoResearch Laboratories. Labelled cells were analysed by epifluorescence or by confocal laser-scanning microscopy (Leica TCS4D). To compare incorporation of rhodamine-actin under various experimental conditions in cells, images were acquired by using equal exposure times (0.4 s) and a linear CCD (charge-coupled device) camera (Princeton Instruments).

RECEIVED 30 MARCH 2000; REVISED 6 MARCH 2001; ACCEPTED 5 APRIL 2001; PUBLISHED 10 JULY 2001.

- Machesky, L. M. *et al.* The mammalian Arp2/3 complex localizes to regions of lamellipodial protrusion and is composed of conserved subunits. *Biochem. J.* **328**, 105–112 (1997).
- Bailly, M. *et al.* Relationship between Arp2/3 complex and the barbed ends of actin filaments at the leading edge of carcinoma cells after epidermal growth factor stimulation. *J. Cell Biol.* **145**, 331–345 (1999).
- Beckerle, M. C. Identification of a new protein localized at sites of cell-substrate adhesion. *J. Cell Biol.* **103**, 1679–1687 (1986).
- Tilney, L. G. & Portnoy, D. A. Actin filaments and the growth, movement, and spread of the intracellular bacterial parasite, *Listeria monocytogenes*. *J. Cell Biol.* **109**, 1597–1608 (1989).
- Machesky, L. M. *et al.* Scar, a WASP-related protein, activates nucleation of actin filaments by the Arp2/3 complex. *Proc. Natl Acad. Sci. USA* **96**, 3739–3744 (1999).
- Rohatgi, R. *et al.* The interaction between N-Wasp and the Arp2/3 complex links Cdc42-dependent signals to actin assembly. *Cell* **97**, 221–231 (1999).
- Mullins, R. D., Heuser, J. A. & Pollard, T. D. The interaction of Arp2/3 complex with actin: Nucleation, high affinity pointed end capping, and formation of branching networks of filaments. *Proc. Natl Acad. Sci. USA* **95**, 6181–6186 (1998).
- Svitkina, T. M. & Borisy, G. C. Arp2/3 complex and actin depolymerizing factor/cofilin in dendritic organization and treadmilling of actin filament array in lamellipodia. *J. Cell Biol.* **145**, 1009–1026 (1999).
- Small, J. V., Herzog, M. & Anderson, K. Actin filament organization in the fish keratocyte lamellipodium. *J. Cell Biol.* **129**, 1275–1286 (1995).
- Domann, E. *et al.* A novel bacterial virulence gene in *Listeria monocytogenes* required for host cell microfilament interaction with homology to the proline-rich region of vinculin. *EMBO J.* **11**, 1981–1990 (1992).
- Kocks, C. *et al.* *L. monocytogenes*-induced actin assembly requires the actA gene product, a surface protein. *Cell* **68**, 521–531 (1992).
- Golsteyn, R. M., Beckerle, M. C., Koay, T. & Friederich, E. Structural and functional similarities between the human cytoskeletal protein zyxin and the ActA protein of *Listeria monocytogenes*. *J. Cell Sci.* **110**, 1893–1906 (1997).
- Crawford, A. W. & Beckerle, M. C. Purification and characterization of zyxin, an 82,000-Dalton component of adherens junctions. *J. Biol. Chem.* **266**, 5847–5853 (1991).
- Beckerle, M. C. Zyxin: zinc fingers at sites of cell adhesion. *BioEssays* **19**, 949–957 (1997).
- Macalma, T. *et al.* Molecular characterization of human zyxin. *J. Biol. Chem.* **271**, 31470–31478 (1996).
- Zumbrunn, J. & Trueb, B. A zyxin-related protein whose synthesis is reduced in virally transformed fibroblasts. *Eur. J. Biochem.* **241**, 657–663 (1996).
- Petit, M. M., Mols, R., Schoenmakers, E. F., Mandahl, N. & Van De Ven, W. J. LPP, the preferred fusion partner gene of HMGIC in lipomas, is a novel member of the LIM protein gene family. *Genomic* **36**, 118–129 (1996).
- Yi, J. & Beckerle, M. The human TRIP6 gene encodes a LIM domain protein and maps to chromosome 7q22, a region associated with tumorigenesis. *Genomics* **49**, 314–316 (1998).

19. Niebuhr, K. *et al.* A novel proline-rich motif present in ActA of *Listeria monocytogenes* and cytoskeletal proteins is the ligand for the EVH1 domain, a protein module present in the Ena/VASP family. *EMBO J.* **16**, 5433–5444 (1997).
20. Drees, B. *et al.* Characterization of the interaction between zyxin and Ena/VASP family of proteins. *J. Biol. Chem.* **275**, 22503–22511 (2000).
21. Lasa, I., David, V., Gouin, E., Marchand, J. P. & Cossart, P. The amino-terminal part of ActA is critical for the actin-based motility of *Listeria monocytogenes*; the central proline-rich region acts as a stimulator. *Mol. Microbiol.* **18**, 425–426 (1995).
22. Smith, G. A., Theriot, J. A. & Portnoy, D. A. The tandem repeat domain in the *Listeria monocytogenes* ActA protein controls the rate of actin-based motility, the percentage of moving bacteria, and the localization of vasodilator-stimulated phosphoprotein and profilin. *J. Cell Biol.* **135**, 647–660 (1996).
23. Loisel, T. P., Boujemaa, R., Pantaloni, D. & Carlier, M. F. Reconstitution of actin-based motility of *Listeria* and *Shigella* using pure proteins. *Nature* **401**, 613–616 (1999).
24. Castellano, F. *et al.* Inducible recruitment of Cdc42 or WASP to a cell-surface receptor triggers actin polymerization and filopodium formation. *Curr. Biol.* **9**, 351–360 (1999).
25. May, R. C. *et al.* The Arp2/3 complex is essential for the actin-based motility of *Listeria monocytogenes*. *Curr. Biol.* **9**, 759–762 (1999).
26. Reinhard, M. *et al.* An α -actinin binding site of zyxin is essential for subcellular zyxin localization and α -actinin recruitment. *J. Biol. Chem.* **274**, 13410–13418 (1999).
27. Cameron, L. A., Footer, M. J., Van Oudenaarden, A. & Theriot, J. A. Motility of ActA protein-coated microspheres driven by actin polymerization. *Proc. Natl Acad. Sci. USA* **96**, 4908–4913 (1999).
28. Noireaux, V. *et al.* Growing an actin gel on spherical surfaces. *Biophys. J.* **278**, 1643–1654 (2000).
29. Welch, M. D., Iwamatsu, A. & Mitchison, T. J. Actin polymerization is induced by Arp2/3 protein complex at the surface of *Listeria monocytogenes*. *Nature* **385**, 265–269 (1997).
30. Lasa, I. *et al.* Identification of two regions in the amino terminal domain of ActA involved in the actin comet tail formation by *Listeria monocytogenes*. *EMBO J.* **16**, 1531–1540 (1997).
31. van Oudenaarden, A. & Theriot, J. A. Cooperative symmetry-breaking by actin polymerization in a model for cell motility. *Nature Cell Biol.* **1**, 493–499 (1999).
32. Zhukarev, V., Ashton, F., Sanger, J. M., Sanger, J. W. & Shuman, H. Organization and structure of actin filament bundles in *Listeria* infected cells. *Cell Motil. Cytoskeleton* **30**, 229–246 (1995).
33. Sechi, A., Wehland, J. & Small, J. V. The isolated comet tail pseudopodium of *Listeria monocytogenes*: a tail of two actin filament populations, long and axial and short and random. *J. Cell Biol.* **137**, 155–167 (1997).
34. Blanchoin, L. *et al.* Direct observation of dendritic actin filament networks nucleated by Arp2/3 complex and WASP/Scar proteins. *Nature* **404**, 1007–1111 (2000).
35. Beckerle, M. C. Spatial control of actin filament assembly: Lessons from *Listeria*. *Cell* **95**, 741–748 (1998).
36. Drees, B., Andrews, K. M. & Beckerle, M. C. Molecular dissection of zyxin function reveals its involvement in cell motility. *J. Cell Biol.* **147**, 1549–1560 (1999).
37. Laurent, V. *et al.* Role of proteins of the Ena-VASP family in actin-based motility of *Listeria monocytogenes*. *J. Cell Biol.* **144**, 1245–1258 (1999).
38. Carlsson, L., Nyström, L.-E., Sundkvist, I., Markey, F. & Lindberg, U. Actin polymerizability is influenced by profilin, a low molecular weight protein in non-muscle cells. *J. Mol. Biol.* **115**, 465–483 (1977).
39. Reinhard, M. *et al.* The proline-rich focal adhesion and microfilament protein VASP is a ligand for profilins. *EMBO J.* **14**, 1583–1589 (1995).
40. Machesky, L. M., Atkinson, S. J., Ampe, C., Vandekerckhove, J. & Pollard, T. D. Purification of a cortical complex containing two unconventional actins from *Acanthamoeba* by affinity chromatography on profilin agarose. *J. Cell Biol.* **127**, 107–115 (1994).
41. Higgs, H. N. & Pollard, T. D. Regulation of actin polymerization by Arp2/3 complex and WASP/Scar proteins. *J. Biol. Chem.* **274**, 32531–32534 (1999).
42. Fradelizi, J., Friederich, E., Beckerle, M. C. & Golsteyn, R. M. Quantitative measurement of proteins by western blotting with Cy5 coupled secondary antibodies. *Biotechniques* **26**, 484–494 (1999).
43. Laurent, V. & Carlier, M.-F. in *Cell Biology: A laboratory manual* (ed Celis, J.) 359–365 (Academic Press, Toronto, 1998).
44. Kreis, T. E., Geiger, B. & Schlessinger, J. Mobility of microinjected rhodamine actin within living chicken gizzard cells determined by fluorescence photobleaching recovery. *Cell* **29**, 835–845 (1982).
45. Friederich, E. *et al.* Targeting of *Listeria monocytogenes* ActA protein to the plasma membrane as a tool to dissect both actin-based cell morphogenesis and ActA function. *EMBO J.* **14**, 2731–2744 (1995).

ACKNOWLEDGEMENTS

We thank L. Cabanié for technical support and members of the Louvard laboratory and M. Beckerle for valuable discussions. We also thank P. Chavrier, P. Cossart, E. Gouin, L. Hoffman, C. Koehler and L. Machesky for generously providing reagents. This work was supported by a Curie Fellowship (to R.M.G. and J.P.), a MENRT fellowship (to J.F. and V.N.), and grants from the Association pour la Recherche sur le Cancer and the Centre National de la Recherche Scientifique (France). Correspondence and requests for materials should be addressed to E.F. and R.M.G. Supplementary Information is available on *Nature Cell Biology's* website (<http://cellbio.nature.com>).

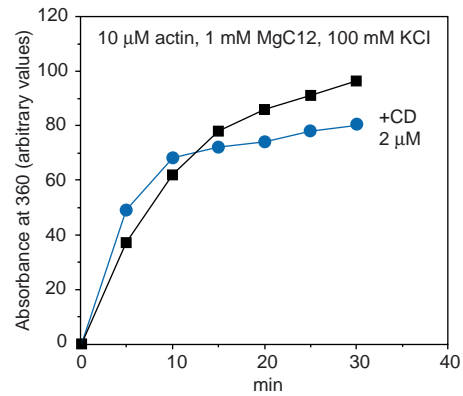
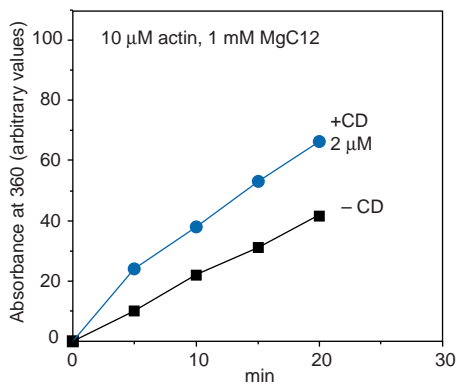


Figure S1 **Effect of cytochalasin D on the ATPase activity of actin during polymerization.** The ATPase activity of actin (10 μM) was measured following a modification (Melki *et al. Biochemistry* **35**,12038–12045; 1996) of a procedure initially developed by Web (*Proc. Natl Sci. USA* **89**, 4884; 1992). This method consists in quantifying Pi release with an enzymatic reaction (EnzChek phosphate assay kit, Molecular Probes). Monomeric actin in G-buffer (see Methods section) was passed over a spin column (Biorad) to remove free nucleotides and then charged

with MgCl₂. Cytochalasin D (CD, 2 μM) in ethanol (circles) or ethanol alone (squares) was added immediately after addition of 1 mM MgCl₂ and 100 mM KCl to induce actin polymerisation. Absorbance was measured at 360 nm (A₃₆₀) in function of time. As determined with a Pi standard, the arbitrary value 100 corresponded to 6 nmoles of Pi per ml. Note that in the presence of KCl, cytochalasin D has very little effect on the initial rate of actin ATPase activity.

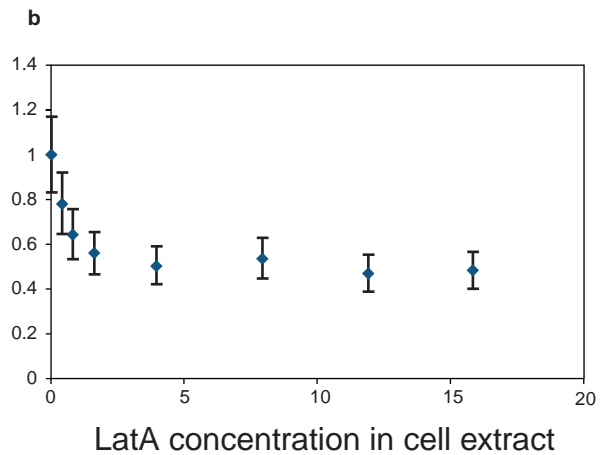
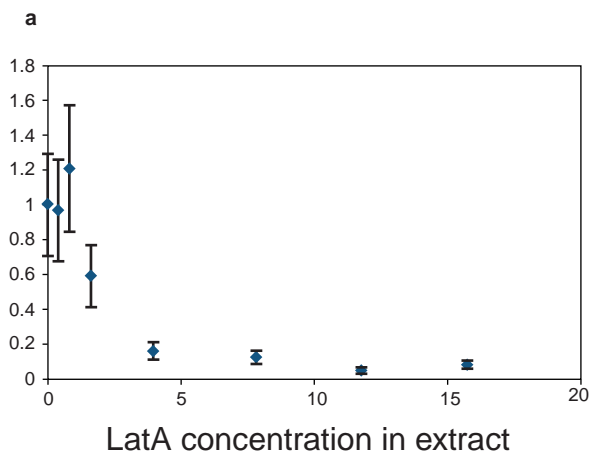


Figure S2 **Inhibition of actin polymerization on the surface of WA or ActA-Pro-beads by increasing concentrations of latrunculin A.** Beads covered with WA (a) or ActA-Pro (b) were incubated in HeLa cell extracts supplemented with 0.5 μM Alexa 568-actin in the presence of increasing concentrations of latrunculin A

(Lat A). Quantification of Alexa 568 fluorescence was performed from images acquired with a linear CCD camera at equal exposure times (see Methods). 10 beads per latrunculin A concentration were analysed. Mean deviations are given. The background fluorescence was not subtracted.

supplementary information

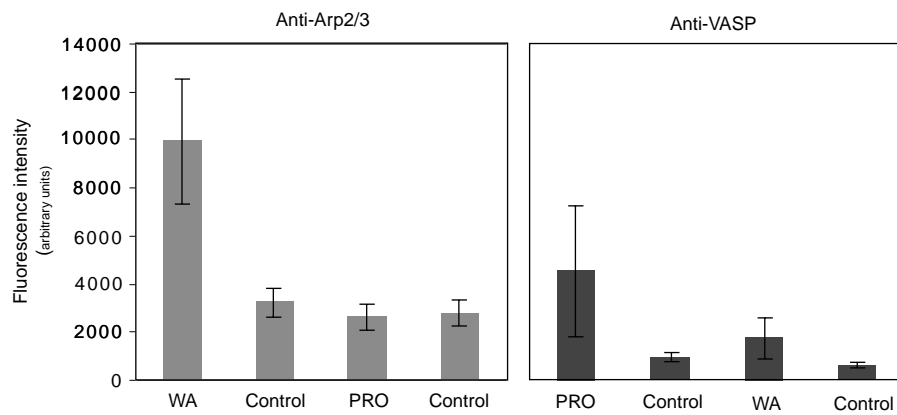


Figure S3 **Quantification of fluorescence associated with WA or ActA-Pro beads immunostained for VASP or Arp3 in the absence of latrunculin A.** ActA-Pro or WA beads were incubated in HeLa cell extracts, and immunostained for VASP or Arp3. Control, no primary antibody. Quantification of fluorescence was per-

formed from images acquired with a linear CCD camera at equal exposure times (see Methods). 10 beads per experimental condition were analysed. Mean deviations are given.